

Supporting Information

## **Modifier-Free Microfluidic Electrochemical Sensor for Heavy Metal Detection**

Liu-Liu Shen,<sup>†</sup> Gui-Rong Zhang,<sup>\*,†</sup> Wei Li,<sup>‡</sup> Markus Biesalski,<sup>‡</sup> and Bastian J.M. Etzold<sup>\*,†</sup>

<sup>†</sup>Ernst-Berl-Institut für Technische und Makromolekulare Chemie, Department of Chemistry, Technische Universität Darmstadt, Alarich-Weiss-Straße 8, 64287 Darmstadt, Germany

<sup>‡</sup>Laboratory of Macromolecular Chemistry and Paper Chemistry, Department of Chemistry, Technische Universität Darmstadt, Petersenstrasse 22, 64287 Darmstadt, Germany

## 1. Assemble of the microfluidic carbon based sensor

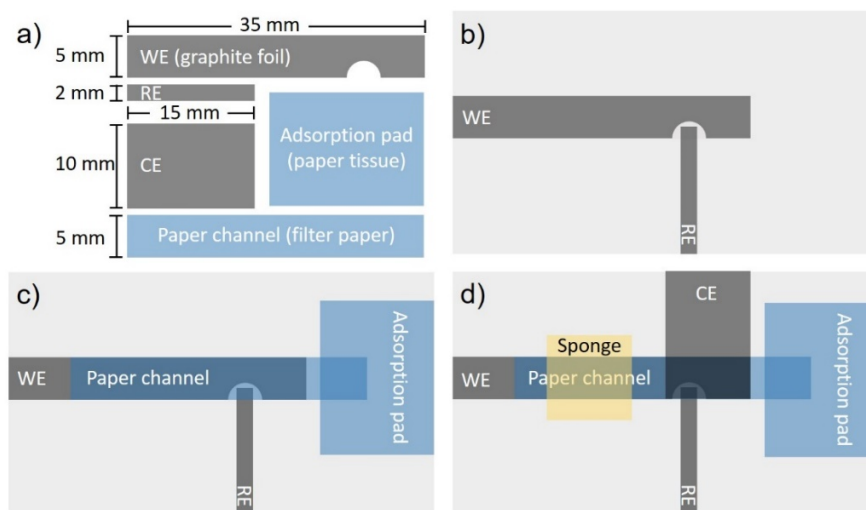


**Figure S1.** Top view of the sensor. (a) Working electrode (WE), reference electrode (RE), counter electrode (CE), paper channel and adsorption pad. (b)-(d) Scheme for the sensor assembling process.

## 2. Optimization of SWASV parameters and detection of heavy metal ions

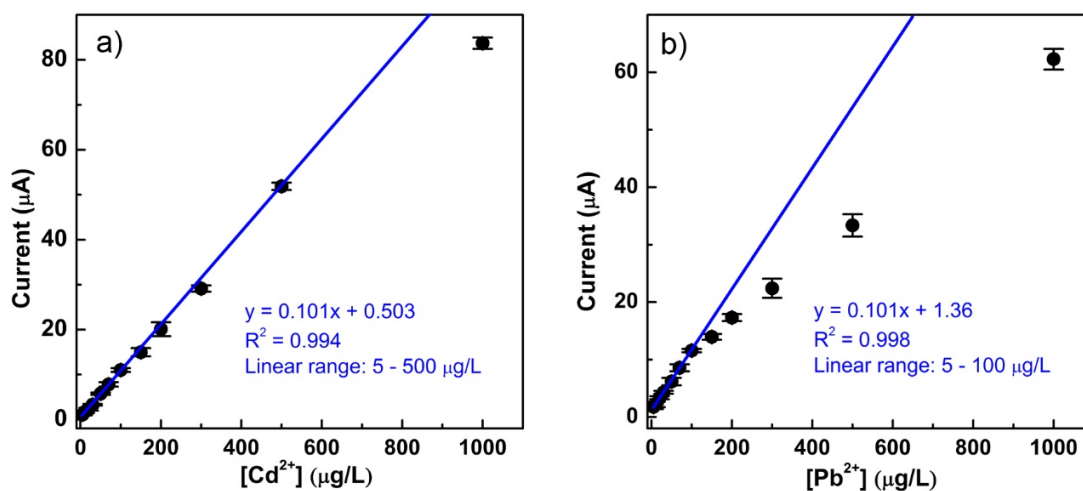


**Figure S2.** The calibration plots for Cd<sup>2+</sup> (a) and Pb<sup>2+</sup> (b) at concentrations ranging from 5 to 1000 µg/L. It can be seen that the linear range for Cd<sup>2+</sup> can be extended up to at least 500 µg/L. However, for Pb<sup>2+</sup>, the current would deviate from the linear plot at concentrations above 100 µg/L.

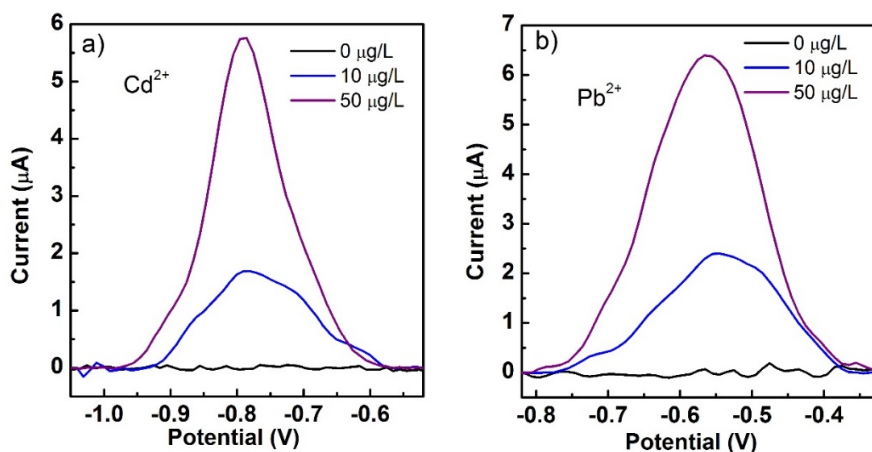


**Figure S3.** Square wave voltammograms for  $\text{Cd}^{2+}$  (a) and  $\text{Pb}^{2+}$  (b) in the commercial mineral water with and without intentionally added  $\text{Cd}^{2+}$  and  $\text{Pb}^{2+}$ .

### 3. Determination of detection limit

Limit of detection (LOD) was calculated by the following equation:<sup>1</sup>

$$DL = \frac{C_1 - C_0}{I_1 - I_0} (3\sigma)$$

Where  $C_1$  is the concentration of the high sample;  $C_0$  is the concentration of the blank;  $I_1$  is the raw intensity of the high sample;  $I_0$  is the raw intensity of the blank;  $\sigma$  is the standard deviation from 4 measurements of the blank.

### 4. Optimization of sensor configuration

Inspired by the ideas from the screen printing sensor, the sensor in our work was initially designed into a 2D configuration, as shown in Figure S6. CE, WE and RE are parallel to each other on the same horizontal plane and analyte flows along the paper channel over the 3 electrodes, as shown in Figure S6 (a). However, this configuration always leads to weak signal (Figure S6 (b)), which may be caused by the high resistance between WE and CE as well as low current efficiency during deposition process.

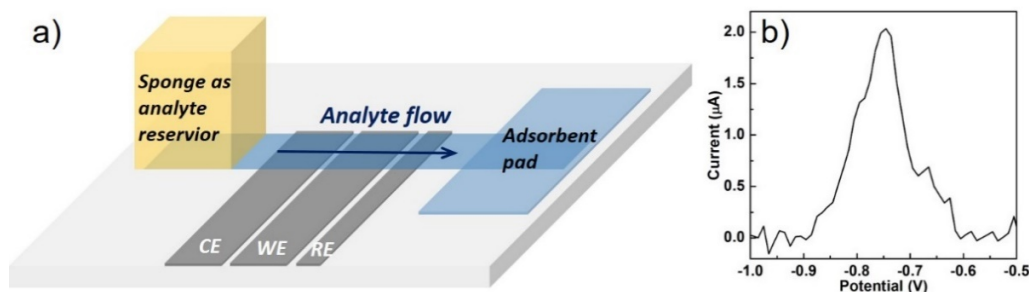


**Figure S4.** (a) Microfluidic carbon based sensor assembled in 2D configuration. (b) Square wave voltammograms for  $100 \mu\text{g/L Cd}^{2+}$  by using 2D structured sensor.

Attempts were also made to directly use the graphite foil as working, counter and reference electrodes in a conventional electrochemical cell containing 20 mL analyte. In this electrochemical cell test, the SWV signal of 100  $\mu\text{g/L Cd}^{2+}$  reaches 12  $\mu\text{A}$ , as shown in Figure S5. This result is comparable that obtained in the microfluidic carbon based sensor (11.5  $\mu\text{A}$ ).

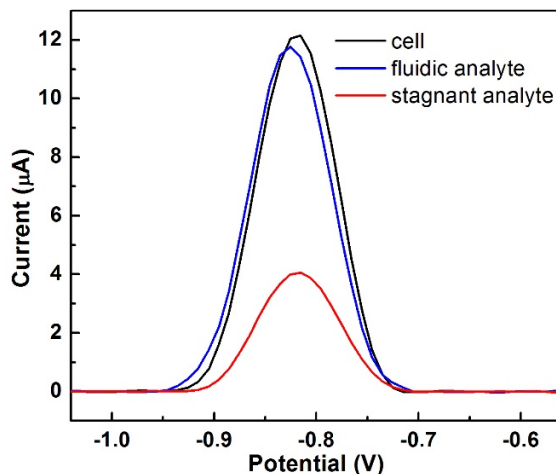


**Figure S5.** Square wave voltammograms for 100  $\mu\text{g/L Cd}^{2+}$  by using electrochemical cell test (black line), fluidic analyte in 3D structured sensor (blue line) and stagnant analyte in 3D structured sensor (red line).

## 5. Effective surface area of WE in the $\mu\text{CS}$

To investigate the effective surface area of WE in the  $\mu\text{CS}$ , we have made attempts to selectively block the area of the WE that is not covered by the counter electrode by using adhesive tapes, to prevent the direct contact of electrolyte with graphite foil (WE) in a hope to reduce the non-Faradic double layer charging current. It turns out that little change in the stripping voltammetry curves can be observed. It seems that the WE surface not covered by the CE is actually playing a minor role in either faradic electrodeposition or non-faradic double layer charging process. This might arise from the small volume of electrolyte confined within the paper channel, the solution resistance increases dramatically with the distance between WE and RE, while the electromigration is also restricted due to the significant distance between the CE and WE area that is not covered by the CE. The effective WE area is around 5 mm  $\times$  5 mm. The effective WE area is around 5 mm  $\times$  5 mm. To investigate the effect of surface area of WE on the sensing performance of the  $\mu\text{CS}$ , we have varied the effective surface area of the WE from 0.10 to 0.75  $\text{cm}^2$  (Figure S6). It turns out that little change in the stripping voltammetry curves can be observed when the area of WE is large than 0.25  $\text{cm}^2$ , which might arise from the too long distance and associated increased solution resistance between the RE and the extended part of WE.

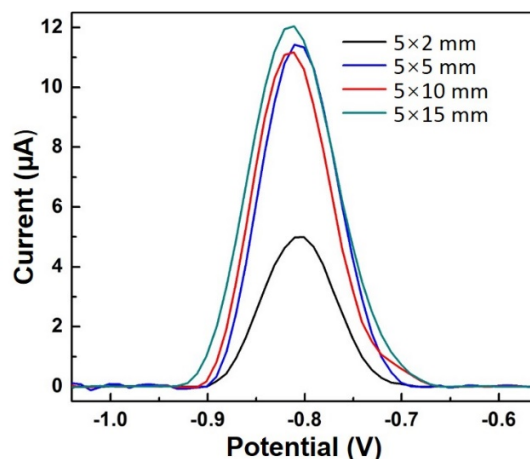


**Figure S6.** SWASV for detecting 100 μg/L Cd<sup>2+</sup> by using μCS with different WE surface areas.

### 6. Sensing performing of Bi<sub>2</sub>O<sub>3</sub> modified working electrode

Bi<sub>2</sub>O<sub>3</sub> modified working electrode was firstly prepared by dropping the mixture ink of Bi<sub>2</sub>O<sub>3</sub> and carbon black (Vulcan XC-72) onto graphite foil.<sup>2</sup> After drying in air, the as prepared WE was tested in a conventional 3-electrode electrochemical cell, with graphite foil as counter and pseudo-reference electrode. One of the main drawbacks of Bi<sub>2</sub>O<sub>3</sub> modified carbon electrode lies in its instability, as shown in Figure S7. After exposing WE for 5 min in air, the anodic stripping voltammetry peak current drops by 43%. The detection activity is only 34% of the initial activity after exposing the WE in air for 30 min.

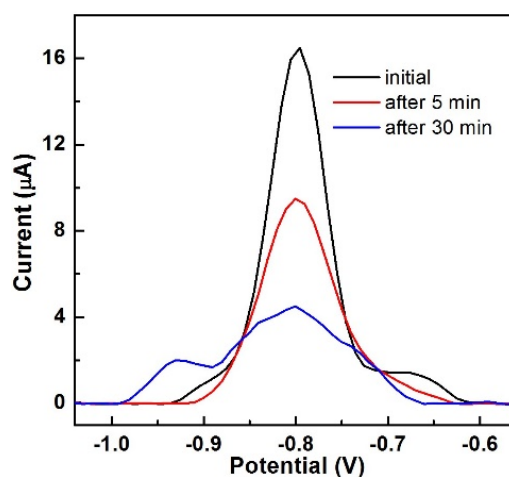


**Figure S7.** Square wave voltammograms by using Bi<sub>2</sub>O<sub>3</sub> modified carbon electrode for Cd<sup>2+</sup> detection.

## 7. Stability of the graphite foils.

In the current work, graphite foils were chosen as the electrode materials for all the sensor fabrications. Before being used as the electrode, the graphite foils have been vigorously cleaned using ethanol and also deionized water under ultrasonication (300 W) for 30 min. It turns out that the graphite foils are rather stable, and no visible dissolution or deformation can be found. We also investigate the storage stability of graphite foil in contacting with analyte solution for 5 days. As shown in Figure S8, a piece of graphite foil was immersed in an analyte solution (0.1 M acetate buffer solution with 100  $\mu\text{g/L}$   $\text{Cd}^{2+}$  and 100  $\mu\text{g/L}$   $\text{Pb}^{2+}$ ), the upper part is not contacting with the solution. We found that after 5 days' storage at room temperature, there's still no visible change or deformation can be found on the graphite foil in contacting with analyte solution, and its appearance is also identical to the part without analyte contacting. These results evidence the superior stability of graphite foils.

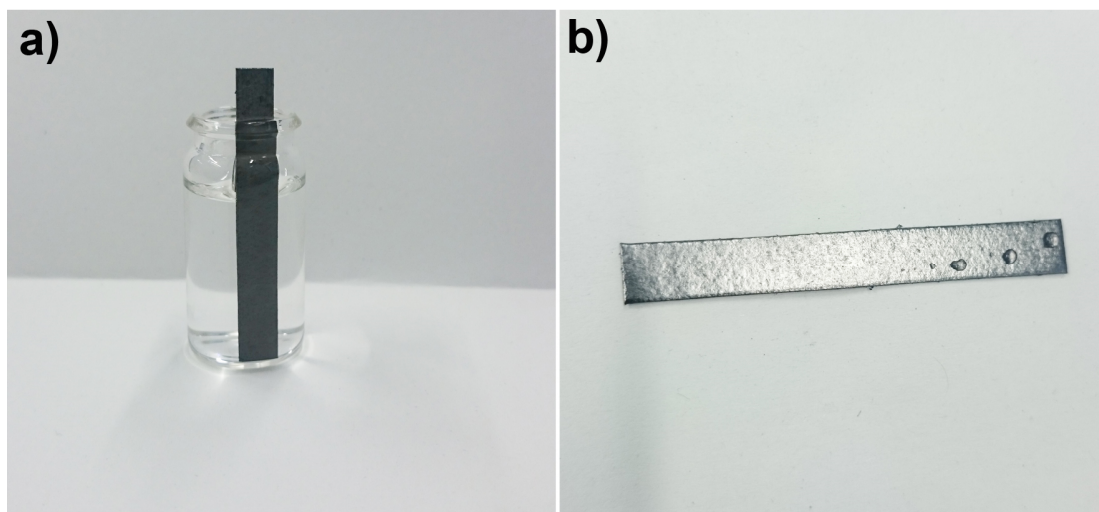


**Figure S8.** (a) Digital photograph of a piece of graphite foil in contact with analyte solution. (b) The graphite foil after contacting with analyte solution for up to 5 days, showing no visible change in structure.

### References:

- (1) Thomsen, V.; Schatzlein, D.; Mercurio, D., Limits of detection in spectroscopy. *Spectroscopy* **2003**, *18*, 112-114.
- (2) Kadara, R. O.; Jenkinson, N.; Banks, C. E., Disposable bismuth oxide screen printed electrodes for the high throughput screening of heavy metals. *Electroanal.* **2009**, *21*, 2410-2414.